Electronic Supplementary Material (ESI) for Materials Chemistry Frontiers.

Supporting Information

High charge carrier storage capacity and wide range X-ray to infrared photon sensing in $LiLuGeO_4:Bi^{3+},Ln^{3+}$ (Ln=Pr, Tb, or Dy) for anti-counterfeiting and information storage applications

Peiran Huang, Zuhui Wen, Yue Yu, Jingyi Xiao, Zhanhua Wei, and Tianshuai Lyu*

Xiamen Key Laboratory of Optoelectronic Materials and Advanced Manufacturing, Institute of Luminescent Materials and Information Displays, College of Materials Science and Engineering, Huaqiao University, Xiamen 361021, China

*Corresponding authors.
E-mail addresses: lv_tianshuai@126.com (T. Lyu).

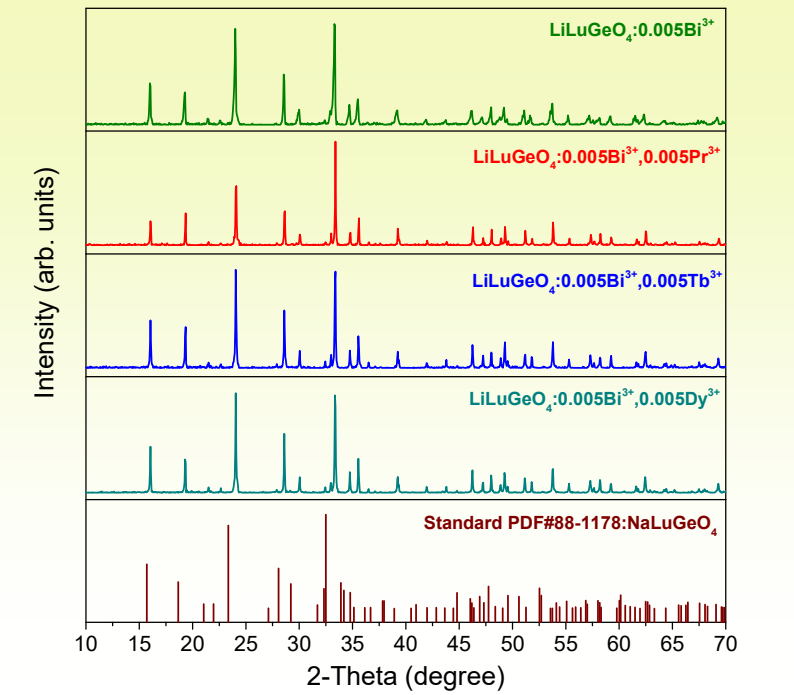

Fig. S1. X-ray diffraction patterns for the prepared $LiLuGeO_4:0.005Bi^{3+}$, $LiLuGeO_4:0.005Bi^{3+},0.005Pr^{3+}$, $LiLuGeO_4:0.005Bi^{3+},0.005Tb^{3+}$, and the $LiLuGeO_4:0.005Bi^{3+}$, $0.005Dy^{3+}$ compounds.

In Fig. S1, the X-ray diffraction pattern of the standard reference $NaLuGeO_4$ compound is shown since $NaLuGeO_4$ and $LiLuGeO_4$ have an identical crystal structure. Fig. S1 shows that the X-ray diffraction patterns of the synthesized $LiLuGeO_4:0.005Bi^{3+}$, $LiLuGeO_4:0.005Bi^{3+},0.005Pr^{3+}$, $LiLuGeO_4:0.005Bi^{3+},0.005Tb^{3+}$, and the $LiLuGeO_4:0.005Bi^{3+}$, $0.005Dy^{3+}$ are almost the same compared with that of the standard reference $NaLuGeO_4$, implying that the synthesized $LiLuGeO_4$ compounds have a single phase.

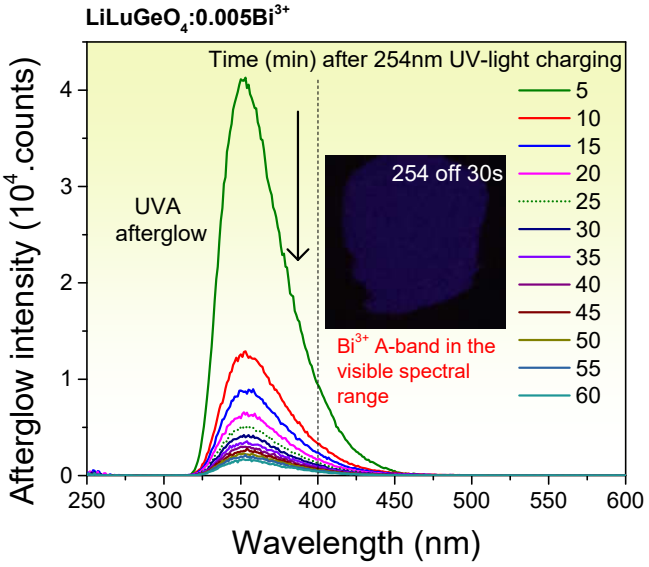

Fig. S2. RT (298 K) isothermal afterglow spectra for $LiLuGeO_4:0.005Bi^{3+}$ after charging by Hg lamp (254 nm UV-light) with a duration of 60s in the dark. An afterglow photograph of $LiLuGeO_4:0.005Bi^{3+}$ recorded at 30s after 254 nm UV-light charging in the dark.

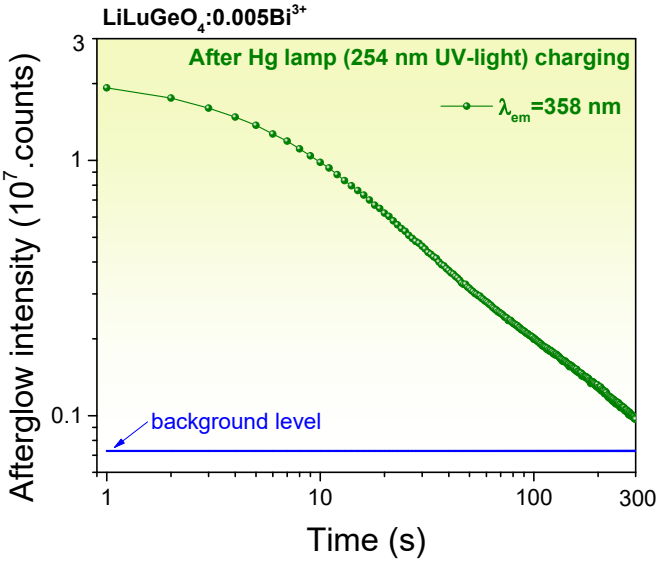

Fig. S3. RT isothermal decay curve of $LiLuGeO_4:0.005Bi^{3+}$ after 254 nm UV-light charging in the dark. The Bi^{3+} 358 nm emission was monitored during this measurement.

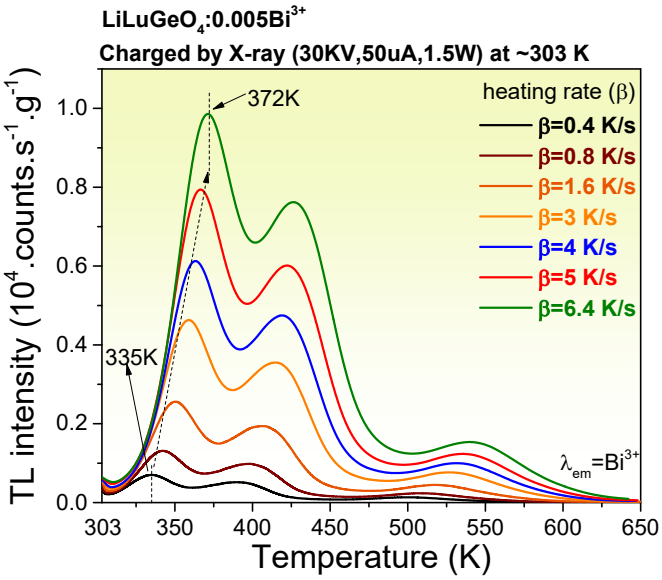

Fig. S4. Thermoluminescence (TL) glow curves of $LiLuGeO_4$:0.005Bi^{3+} measured at different heating rate from β=0.4 K/s until β=6.4 K/s after 200s charging in the dark. The Bi^{3+} emissions were monitored during TL-readout.

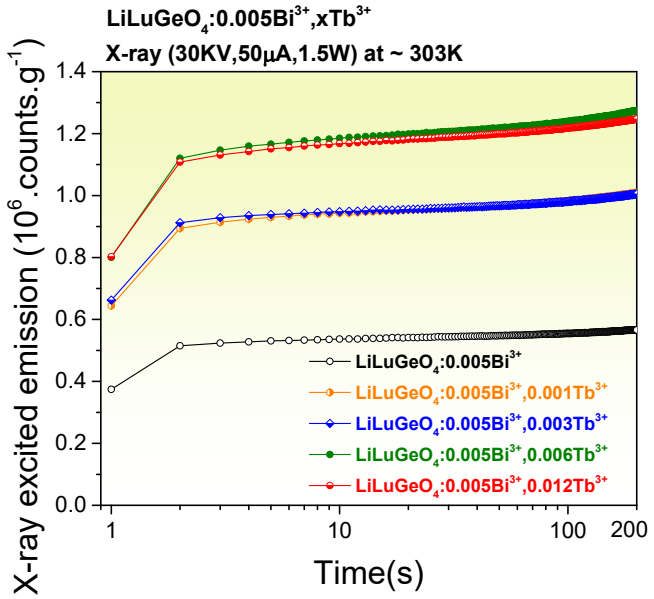

Fig. S5. X-ray excited emission intensities as a function of time for the synthesized $LiLuGeO_4$:0.005Bi^{3+},xTb^{3+} (x=0 until 0.012) storage phosphors. The emission from 300 to 750 nm was monitored. A constant sample mass of 0.0300 g was utilized and the emission intensity was corrected by the sample mass.

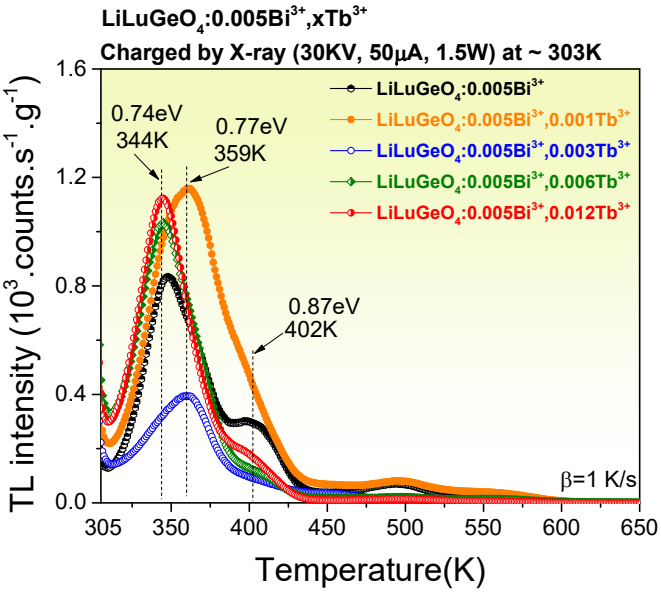

Fig. S6. TL glow curves measured at a heating rate of 1 K/s for the $LiLuGeO_4:0.005Bi^{3+},xTb^{3+}$ (x=0 until 0.012) storage phosphors after X-ray charging.

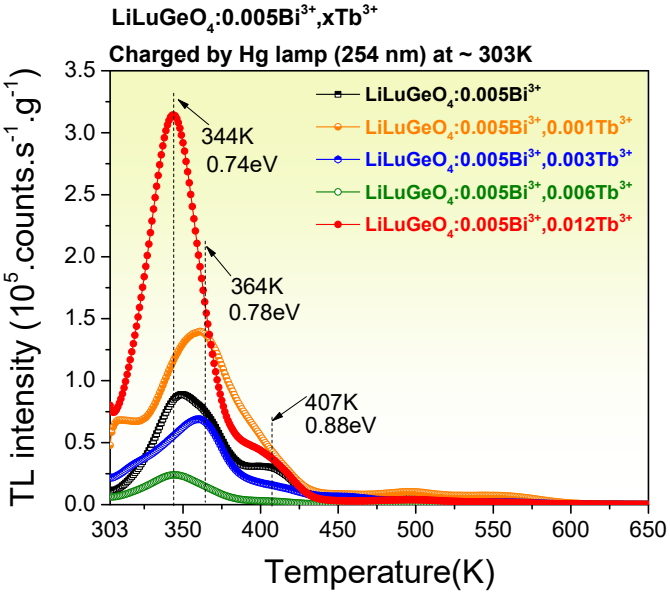

Fig. S7. TL glow curves recorded at a heating rate of 1 K/s for the $LiLuGeO_4:0.005Bi^{3+},xTb^{3+}$ (x=0 until 0.012) storage phosphors after 254 nm UV-light charging in the dark.

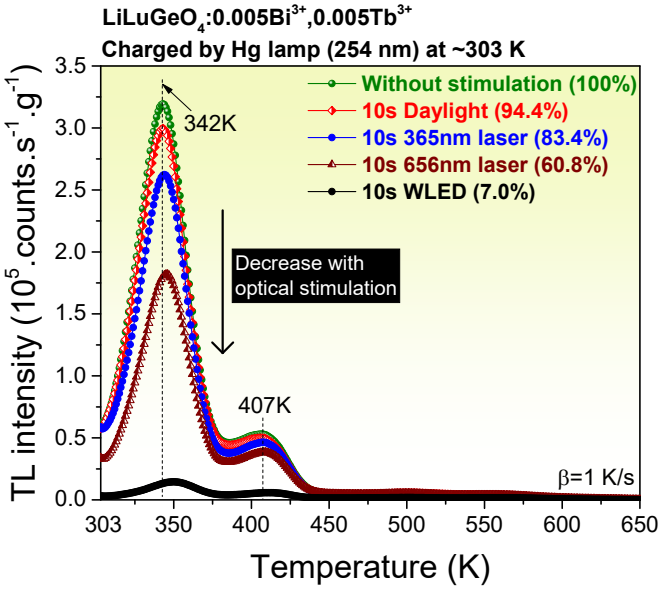

Fig. S8. TL glow curves of $LiLuGeO_4$:0.005Bi^{3+},0.005Tb^{3+} after first exposure to 254 nm UV-light and then followed by different energy photon stimulation with a duration of 10s in the dark. The utilized heating rate was 1 K/s and the emissions of Bi^{3+} and Tb^{3+} were monitored during TL-readout. The ratios of the integrated TL intensities with additional optical stimulation to that of without additional optical stimulation are shown as percentages in the legend.

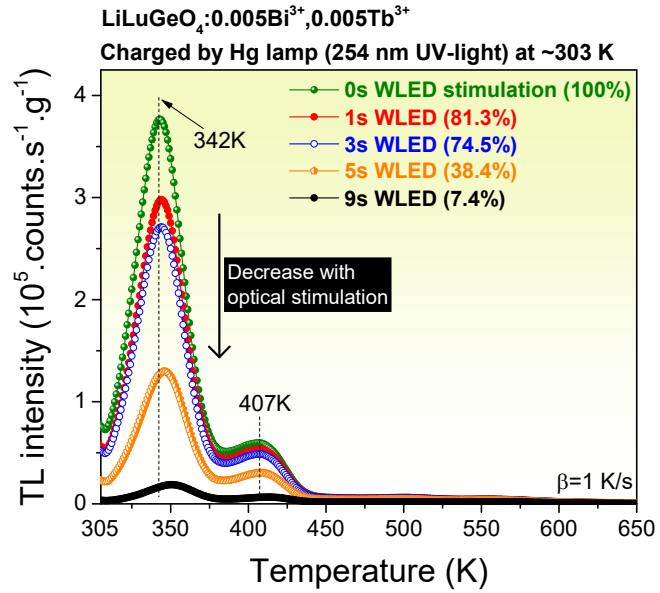

Fig. S9. TL glow curves measured at a heating rate of 1 K/s for $LiLuGeO_4$:0.005Bi^{3+}, 0.005Tb^{3+} after first exposure to 254 nm UV-light and then followed by WLED stimulation with different duration from 0s until 9s in the dark. The ratios of the integrated TL intensities with additional optical stimulation to that of without additional optical stimulation are shown as percentages in the legend.

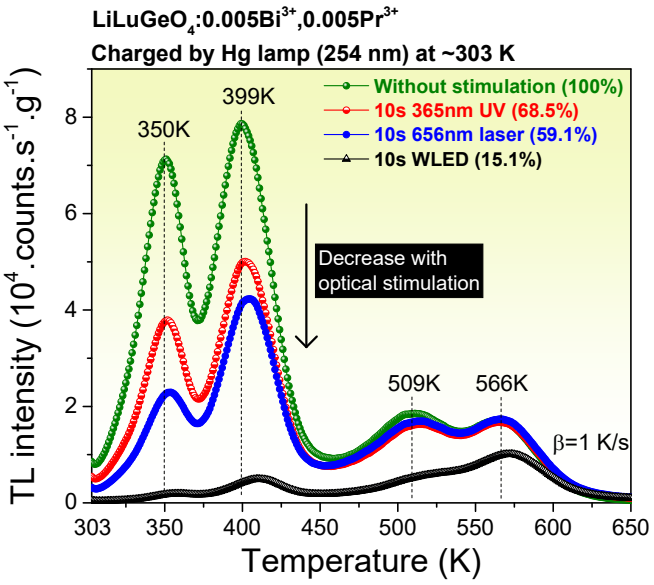

Fig. S10. TL glow curves measured at a heating of 1 K/s for $LiLuGeO_4$:0.005Bi^{3+},0.005Pr^{3+} after 254 nm UV-light charging and then followed by different energy photon stimulation in the dark. The Bi^{3+} and Pr^{3+} emissions were monitored during TL-readout. The ratios of the integrated TL intensities with additional optical stimulation to that of without additional optical stimulation are shown as percentages in the legend.

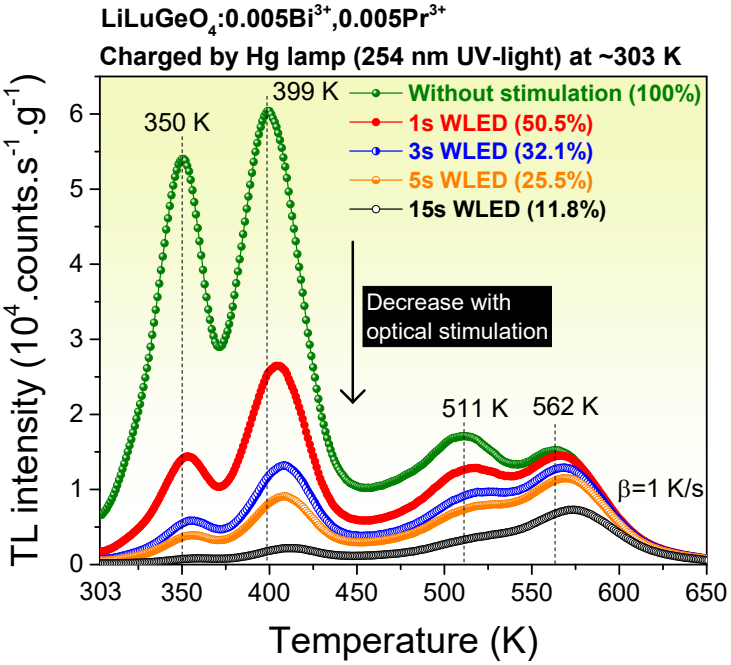

Fig. S11. TL glow curves measured at β=1 K/s for $LiLuGeO_4$:0.005Bi^{3+},0.005Pr^{3+} after 254 nm UV-light charging and then followed by WLED stimulation with different duration from 0s until 15s in the dark. The ratios of the integrated TL intensities with additional optical stimulation to that of without additional optical stimulation are shown as percentages in the legend.

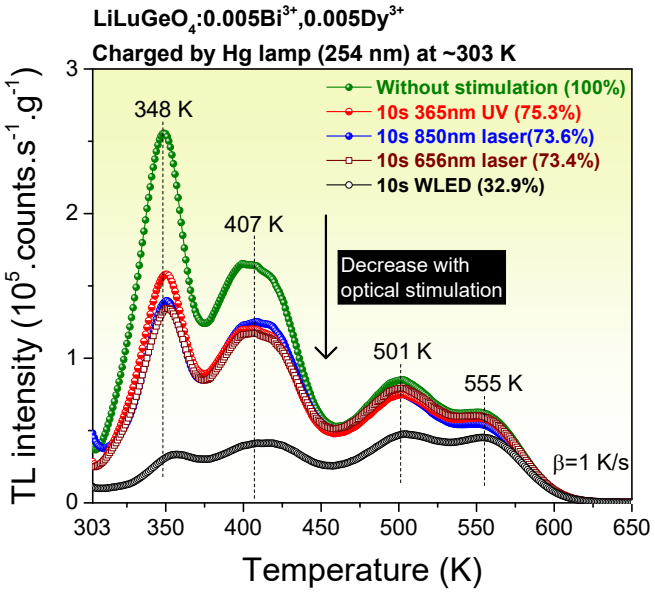

Fig. S12. TL glow curves of $LiLuGeO_4$:0.005Bi^{3+},0.005Dy^{3+} after 254 nm UV-light charging and then followed by different energy photon stimulation for 10s. The ratios of the integrated TL intensities with additional optical stimulation to that of without additional optical stimulation are shown as percentages in the legend.

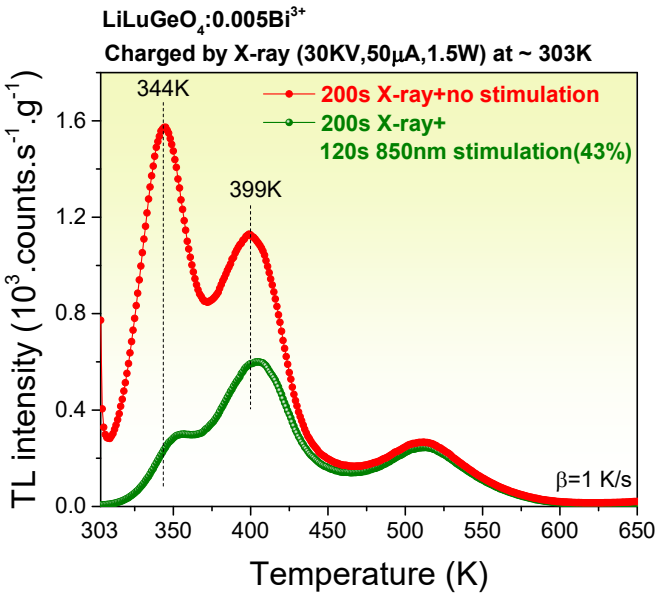

Fig. S13. TL glow curves of $LiLuGeO_4$:0.005Bi^{3+} recorded at a heating rate of 1 K/s after 200s X-ray charging and the followed by 850 nm infrared laser stimulation with a duration of 120s. The Bi^{3+} emissions were monitored during the TL-readout. The ratio of the integrated TL intensity with additional optical stimulation to that of without additional optical stimulation is shown as a percentage in the legend.

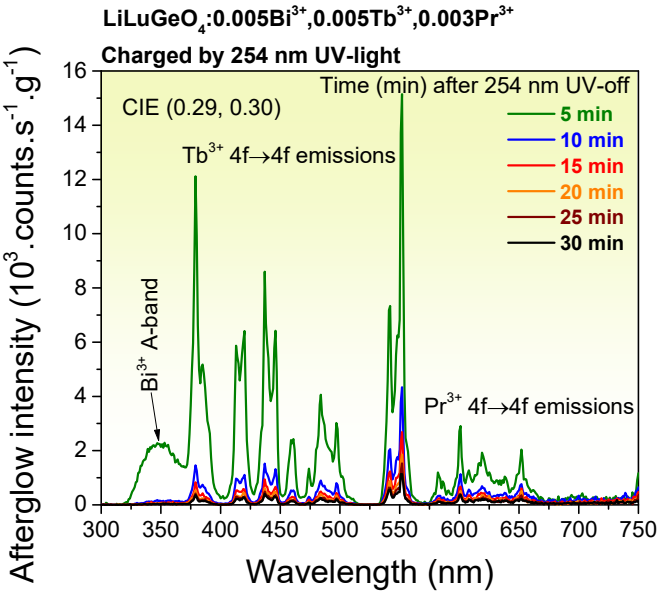

Fig. S14. RT isothermal afterglow spectra of $LiLuGeO_4$:0.005Bi^{3+},0.005Tb^{3+},0.003Pr^{3+} after Hg lamp (254 nm UV-light) charging in the dark.

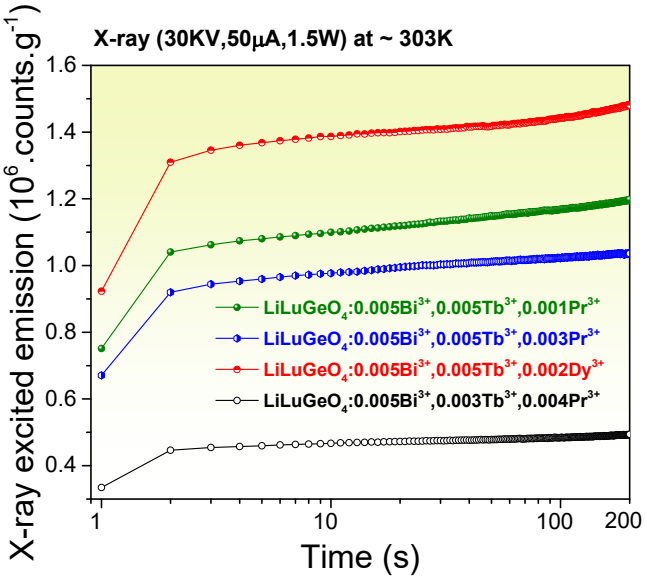

Fig. S15. X-ray excited emission intensities of the Bi^{3+}, Tb^{3+}, Pr^{3+}, or Dy^{3+} doped $LiLuGeO_4$ storage phosphors as a function of time in the dark. The emission intensities were corrected by the sample mass.

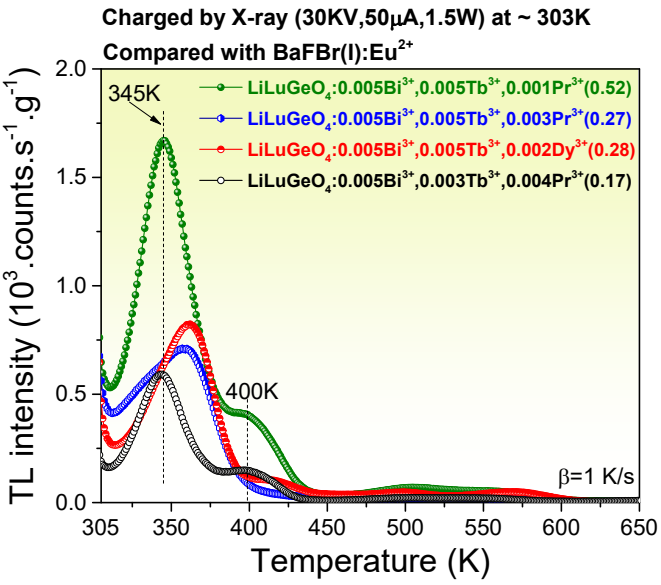

Fig. S16. TL glow curves measured at a heating rate of 1 K/s for the Bi^{3+}, Tb^{3+}, Pr^{3+}, or Dy^{3+} doped $LiLuGeO_4$ storage phosphors after exposure to X-rays. The ratios of the integrated TL intensities from 305 to 650 K of the Bi^{3+}, Tb^{3+}, Pr^{3+}, or Dy^{3+} doped $LiLuGeO_4$ to that of the commercial $BaFBr(I):Eu^{2+}$ are shown in the legend.

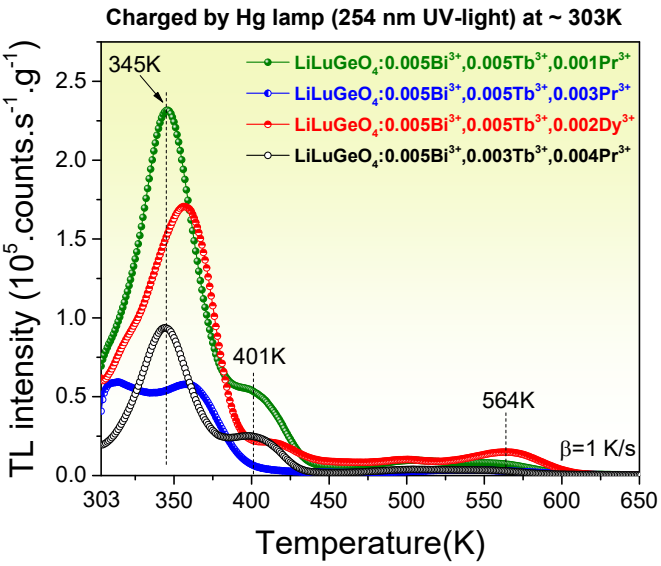

Fig. S17. TL glow curves for the Bi^{3+}, Tb^{3+}, Pr^{3+}, or Dy^{3+} doped $LiLuGeO_4$ storage phosphors measured at a heating rate of 1 K/s after 254 nm UV-light charging in the dark.

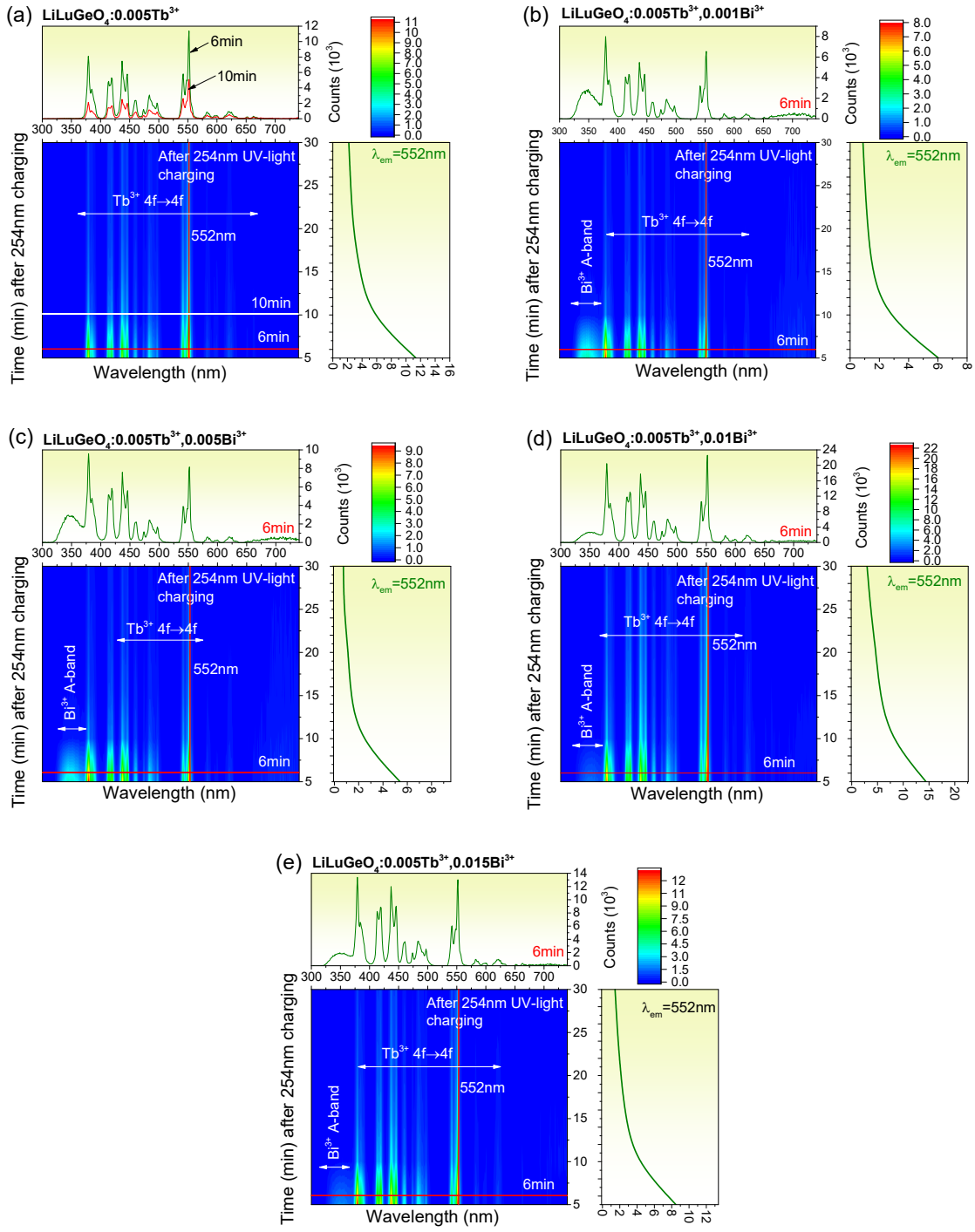

Fig. S18. 2D contour plots of room temperature (297 K) isothermal decay spectra as a function of time after Hg lamp (254 nm UV-light) charging for (a) $LiLuGeO_4:0.005Tb^{3+}$, (b) $LiLuGeO_4:0.005Tb^{3+},0.001Bi^{3+}$, (c) $LiLuGeO_4:0.005Tb^{3+},0.005Bi^{3+}$, (d) $LiLuGeO_4:0.005Tb^{3+}$, $0.01Bi^{3+}$, and (e) $LiLuGeO_4:0.005Tb^{3+},0.015Bi^{3+}$ in the dark.

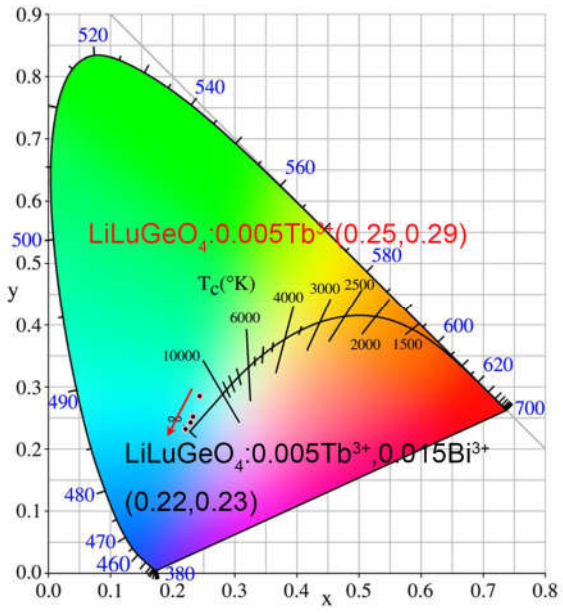

Fig. S19. Colour coordinates for the RT isothermal afterglow spectra recorded at 5 minutes after 254 nm UV-light charging for $LiLuGeO_4$:0.005Tb^{3+},yBi^{3+} (y=0 until 0.015).

Movies

Movie 1: Demonstration of the afterglow logo of " T. Lyu" in the dark after Hg lamp (254 nm UV-light) charging.

Movie 2: Detailed illustration of colour-tailorable afterglow logo of "T. Lyu" in the dark after 254 nm UV-light charging.

Movie 3: Appearance of the "T. Lyu" logo during 254 nm UV-light illumination.

Movie 4: Afterglow from the optimized $LiLuGeO_4$:0.005Bi^{3+},0.012Tb^{3+} storage phosphor after 254 nm UV-light charging in the dark.

Movie 5: Afterglow from the $LiLuGeO_4$:0.005Bi^{3+},0.005Tb^{3+},0.003Pr^{3+} after 254 nm UV-light charging in the dark.